Morphogenesis and Crystallization of Bi_2S_3 Nanostructures by an Ionic Liquid-Assisted Templating Route: Synthesis, Formation Mechanism, and Properties

Jie Jiang,[†] Shu-Hong Yu,*[,†] Wei-Tang Yao,[†] Hui Ge,[‡] and Guang-Zhao Zhang[‡]

Division of Nanomaterials & Chemistry, Hefei National Laboratory for Physical Sciences at Microscale, Structural Research Laboratory of CAS, Department of Materials Science and Engineering, and Department of Chemical Physics, University of Science and Technology of China, Hefei 230026, People's Republic of China

Received July 25, 2005. Revised Manuscript Received September 27, 2005

An ionic liquid 1-butyl-3-methylimidazolium tetrafluoroborate ([BMIM][BF_4]) solution system has been designed for the morphogenesis and crystallization of Bi_2S_3 nanostructures at low temperature and ambient atmosphere. Uniform Bi_2S_3 flowers with a size of 3−5 μm, which are composed of nanowires with a diameter of 60−80 nm, can be prepared in large scale by the template effect of the ionic liquid solution, in which vesicles are formed as confirmed by laser light scattering (LLS) analysis. The formation mechanism of the flowers has been proposed. With prolonged aging time, the flowerlike structures tend to become loose and fall off from the mother flowers, and finally the individual nanowires will form. The results demonstrated that the shape evolution and phase transformation strongly depend on the reaction conditions, such as pH value, reaction temperature, and reaction time. This reaction system could be extended for the morphogenesis of other inorganic nanomaterials with novel morphology and complex form.

1. Introduction

Recently ionic liquids (ILs), as a green solvent, have gained a great deal of both academic and industrial attention as a new class of compounds for a potential effective green replacement of conventional organic solvents for long-lasting development of human society.[1] Due to their low melting points below 100 °C, sometimes as low as −96 °C, and possessing wide liquidus, even in excess of 400 °C, ILs are good solvents for a wide range of inorganic, organic, and polymer materials, and usual combinations of these individual reagents can be brought into the same phase.[2] Especially, ILs as a new reaction medium have many advantages in the inorganic nanomaterial synthetic field. Novel nanostructures can be produced by selecting suitable IL reaction systems; TiO_2,[3] metal nanoparticles,[4] Te nanorods,[5] Si,[6] CoPt nanorods,[7] and porous silica[8] have been synthesized as reported recently. The latest developments of IL as a reaction medium for inorganic nanomaterials have received much attention and could offer many opportunities and challenges for the synthesis of nanoparticles with unique shape and structures.[9] Yet this new kind of reaction medium still needs to be explored more widely for other inorganic systems.

The preparation and controlled fabrication of nanostructured materials with functional properties have attracted more and more attention in recent years for their properties (optical, electrical, mechanical, chemical, etc.).[10] Semiconductor nanoparticles have been identified as important materials with potential applications in a wide range of fields.[11] Main-group

* Corresponding author: fax + 86 551 3603040; e-mail shyu@ustc.edu.cn.
[†] Division of Nanomaterials & Chemistry, Hefei National Laboratory for Physical Sciences at Microscale, Structural Research Laboratory of CAS, Department of Materials Science and Engineering.
[‡] Department of Chemical Physics.

(1) (a) Seddon, K. R. *Nat. Mater.* **2003**, *2*, 363. (b) Welton, T. *Chem. Rev.* **1999**, *99*, 2071. (c) Wasserscheid, P.; Keim, W. *Angew. Chem., Int. Ed.* **2000**, *39*, 3773. (d) Wasserscheid, P.; Welton, T. *Ionic liquids in synthesis*; Wiley−VCH: Weinheim, Germany, 2002. (e) Adam, D. *Nature* **2000**, *407*, 938. (f) Freemantle, M. *Chem. Eng. News* **2000**, *78*, 37. (g) Carmichael, A. J.; Hardacre, C.; Holbrey, J. D.; Nieuwenhuyzen, M.; Seddon, K. R. *Proc. Electrochem. Soc.* **2000**, *99*, 209.
(2) (a) Seddon, K. R.; Stark, A.; Torres, M. J. *Pure Appl. Chem.* **2000**, *72*, 2275. (b) Walden, P. *Izv. Imp. Akad. Nauk, Ser. 6* **1914**, *8*, 1800.
(3) (a) Nakashima, T.; Kimizuka, N. *J. Am. Chem. Soc.* **2003**, *125*, 6386. (b) Yoo, K.; Choi, H.; Dionysiou, D. D. *Chem. Commun.* **2004**, 2000. (c) Zhou, Y.; Antonietti, M. *J. Am. Chem. Soc.* **2003**, *125*, 14960.
(4) (a) Huang, J.; Jiang, T.; Han, B. X.; Gao, H. X.; Chang, Y. H.; Zhao, G. Y.; Wu, W. Z. *Chem. Commun.* **2003**, 1654. (b) Dupont, J.; Fonseca, G. S.; Umpierre, A. P.; Fichtner, P. F. P.; Teixeira, S. R. *J. Am. Chem. Soc.* **2002**, *124*, 4228. (c) Fonseca, G. S.; Umpierre, A. P.; Fichtner, P. F. P.; Teixeira, S. R.; Dupont, J. *Chem.-Eur. J.* **2003**, *9*, 3263. (c) Fonseca, G. S.; Scholten, J. D.; Dupont, J. *Synlett* **2004**, 1525. (d) Scheeren, C. W.; Machado, G.; Dupont, J.; Fichtner, P. F. P.; Texeira, S. R. *Inorg. Chem.* **2003**, *42*, 4738. (e) Kim, K. S.; Demberelnyamba, D.; Lee, H. *Langmuir* **2004**, *20*, 556. (f) Mu, X. D.; Evans, D. G.; Kou, Y. A. *Catal. Lett.* **2004**, *97*, 151. (g) Zhang, S. M.; Zhang, C. L.; Zhang, J. W.; Zhang, Z. J.; Dang, H. X.; Wu, Z. S.; Liu, W. M. *Acta Phys.-Chim. Sin.* **2004**, *20*, 554. (h) Zhang, S. M.; Zhang, C. L.; Wu, Z. S.; Zhang, Z. J.; Dang, H. X.; Liu, W. M.; Xue, Q. J. *Acta Chim. Sin.* **2004**, *62*, 1443. (i) Endres, F.; Bukowski, M.; Hempelmann, R.; Natter, H. *Angew. Chem.* **2003**, *115*, 3550; *Angew. Chem., Int. Ed.* **2003**, *42*, 3428.
(5) Zhu, Y. J.; Wang, W. W.; Qi, R. J.; Hu, X. L. *Angew. Chem., Int. Ed.* **2004**, *43*, 1410.
(6) Abedin, S. Z. El.; Borissenko, N.; Endres, F. *Electrochem. Commun.* **2004**, *6*, 510.
(7) Wang, Y.; Yang, H. *J. Am. Chem. Soc.* **2005**, *127*, 5316.
(8) (a) Zhou, Y.; Schattka, J. H.; Antonietti, M. *Nano Lett.* **2004**, *4*, 477. (b) Zhou, Y.; Antonietti, M. *Chem. Mater.* **2004**, *16*, 544. (c) Zhou, Y.; Antonietti, M. *Adv. Mater.* **2003**, *15*, 1452.
(9) Zhou, Y. *Curr. Nanosci.* **2005**, *1*, 35.
(10) Caruso, F. *Adv. Mater.* **2001**, *13*, 11.

10.1021/cm051632t CCC: $30.25 © 2005 American Chemical Society
Published on Web 11/05/2005

Scheme 1. Illustration of Synthetic Procedures for 1-Butyl-3-methylimidazolium Tetrafluoroborate ([BMIM][BF_4])

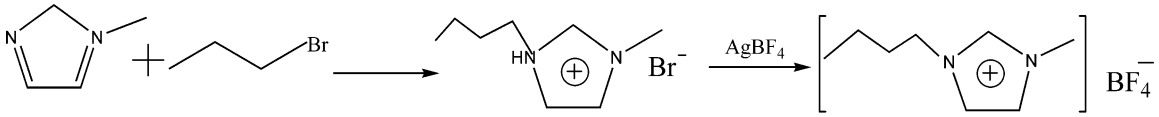

1.1-butyl-3-methyl-imidazolium-bromide

metal chalcogenides such as $A^V{}_2B^{VI}{}_3$ (where A = As, Sb, Bi and B = S, Se, Te) as significant semiconductors have many applications in television cameras with photoconducting targets, thermoelectric devices, optoelectronic devices, and IR spectroscopy.[12] As a direct band-gap material with an E_g of 1.3 eV,[13] Bi_2S_3 has found applications in photodiode arrays or photovoltaics.[14] Shape control and exploration of novel methods for self-assembling or surface-assembling molecules or colloids to generate Bi_2S_3 nanomaterials with controlled morphologies and unique properties have been sought in recent years. Usually, this material was traditionally synthesized by high-temperature approaches such as direct element reaction in a quartz vessel at high temperature,[15] the chemical deposition method,[16] and the thermal decomposition method.[17] Previously, our group has developed hydrothermal[18] and solvothermal methods,[19,20] respectively, for the synthesis of Bi_2S_3 nanorods, nanowires, and nanobelts. Biomolecules such as glutathione[21] and lysozyme[22] have been used as additives in hydrothermal synthesis methods for the synthesis of Bi_2S_3 snowflakelike structures and nanowires. Other methods include a sonochemical method[23] and a microwave irradiation method.[24] Recently, Sigman and Korgel[25] reported a novel solventless phase transfer method for the formation of Bi_2S_3 nanorods, nanowires, and nanofabric. Although there is a report on the use of microwave-assisted synthesis of sulfide M_2S_3 nanorods in ionic liquid system at 190 °C, yet there are other additives, such as ethylene glycol (EG) and ethanolamine, which have also been used in such reaction systems.[26]

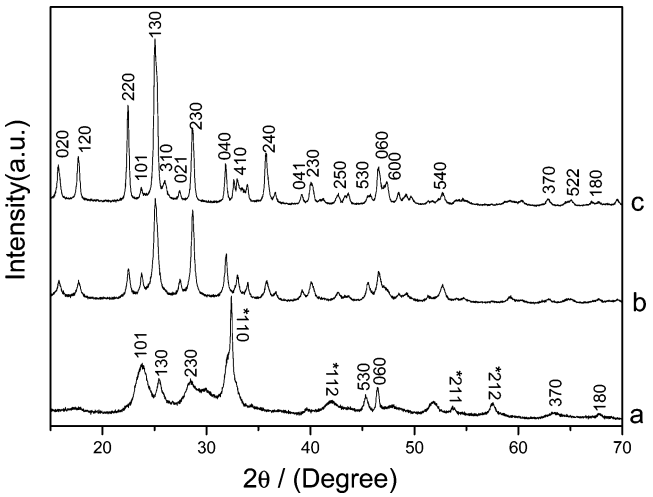

Figure 1. XRD patterns of Bi_2S_3 nanostructures obtained after reaction at 120 °C for different times: (a) 1 h, (b) 3 h, (c) 20 h. Asterisks denote BiOCl phase.

In this paper, we report a new method for the morphogenesis of Bi_2S_3 nanostructures using an ionic liquid, 1-butyl-3-methylimidazolium tetrafluoroborate ([BMIM][BF_4]), as a reaction medium. Uniform Bi_2S_3 nanoflowers composed of individual nanowires can be produced, based on the template effects of the formation of micelles confirmed by light scattering measurement, showing that the mixed medium of an ionic liquid and water can be used for the morphogenesis of Bi_2S_3 nanostructures. To our best knowledge, this is first report for the synthesis of Bi_2S_3 flowers in an ionic liquid under mild reaction conditions.

2. Experimental Section

2.1. Synthesis of ILs. All chemicals were purchased and used without further purification. The ionic liquid 1-butyl-3-methylimidazolium tetrafluoroborate ([BMIM][BF_4]) was synthesized at 90 °C by use of 1-methylimidazolium and $AgBF_4$ as reactants.[27] The process is shown in Scheme 1.

2.2. Synthesis of Bi_2S_3 Nanostructures in ILs. In a typical synthesis, 0.8 mL of 0.2 M acetothioamide and 0.4 mL of 0.2 M $BiCl_3$ solution are mixed together with 3 mL of ILs in a small jar (entire volume is 10 mL), and then the mixture underwent ultrasonic treatment for about 5 min (final concentration of Bi^{3+} is 20 mmol/

(11) (a) Henglein, A. *Chem. Rev.* **1989**, *89*, 1861. (b) Steigerwald, M. L.; Brus, L. E. *Acc. Chem. Res.* **1990**, *23*, 183. (c) Weller, H. *Angew. Chem., Int. Ed. Engl.* **1993**, *32*, 41. (d) Weller, H. *Adv. Mater.* **1993**, *5*, 88. (e) Hagfeldt, A.; Gratzel, M. *Chem. Rev.* **1995**, *95*, 49. (f) Fendler, J. H.; Meldrum, F. C. *Adv. Mater.* **1995**, *95*, 607. (g) Alivisatos, A. P. *Science* **1996**, *271*, 933.
(12) Arivuoli, D.; Gnanam, F. D.; Ramasamy, P. *J. Mater. Sci. Lett.* **1988**, *7*, 711.
(13) (a) Black, J.; Conwell, E. M.; Seigle, L.; Spencer, C. W. *J. Phys. Chem. Solids* **1957**, *2*, 240. (b) Nomura, R.; Kanaya, K.; Matsuda, H. *Bull. Chem. Soc. Jpn.* **1989**, *62*, 939.
(14) (a) Miller, D. D.; Heller, A. *Nature* **1976**, *262*, 280. (b) Mahapatra, P. K.; Roy, C. B. *Sol. Cells* **1982/83**, *7*, 225. (c) Schoijet, J. M. *Sol. Energy Mater.* **1979**, *1*, 43. (d) Farrugia, L. J.; Lawlor, F. J.; Norman, N. C. *Polyhedron* **1995**, *14*, 311. (e) Nayak, B. B.; Acharya, H. N.; Mitra, G. B.; Mathur, B. K. *Thin Solid Films* **1983**, *105*, 17. (f) Pawar, S. H.; Bhosale, P. N.; Uplane, M. D.; Tanhankar, S. *Thin Solid Films* **1983**, *110*, 165.
(15) Kaito, C.; Saito, Y.; Fujia, K. *J. Cryst. Growth* **1998**, *94*, 967.
(16) (a) Biswas, S.; Mondal, A.; Mukherjee, D.; Pramanik, P. *J. Electrochem. Soc.* **1986**, *133*, 48. (b) Yesugade, N. S.; Lokhande, C. D.; Bhosale, C. H. *Thin Solid Films* **1995**, *263*, 145. (c) Engelken, R. D.; Ali, S.; Chang, L. N.; Brinkley, C.; Turner, K.; Hester, C. *Mater. Lett.* **1990**, *10*, 264. (d) Ye, C.; Meng, G.; Jiang, Z.; Wang, Y.; Wang, G.; Zhang, L. *J. Am. Chem. Soc.* **2002**, *124*, 15180.
(17) (a) Pramanik, P.; Bhattachrga, S. *J. Mater. Sci. Lett.* **1987**, *6*, 1105. (b) Desai, J. D.; Lokhande, C. D. *Ind. J. Pure Appl. Phys.* **1993**, *31*, 152. (c) Lokhande, C. D.; Yermune, V.S.; Pawar, S. H. *J. Electrochem. Soc.* **1998**, *135*, 1852.
(18) Yu, S. H.; Yang, J.; Wu, Y. S.; Han, Z. H.; Xie, Y.; Qian, Y. T. *Mater. Res. Bull.* **1998**, *33*, 1661.
(19) (a) Yu, S. H.; Qian, Y. T.; Shu, L.; Xie, Y.; Yang, L.; Wang, C. S. *Mater. Lett.* **1998**, *35*, 116. (b) Yu, S. H.; Shu, L.; Yang, J. A.; Han, Z. H.; Qian, Y. T.; Zhang, Y. H. *J. Mater. Res.* **1999**, *14*, 4157. (c) Liu, Z. P.; Peng, S.; Xie, Q.; Hu, Z. K.; Yang, Y.; Zhang, S. Y.; Qian, Y. T. *Adv. Mater.* **2003**, *15*, 936.
(20) Xie, G.; Qiao, Z.-P.; Zeng, M.-H.; Chen, X.-M.; Gao, S.-L. *Cryst. Growth Des.* **2004**, *4*, 513.
(21) Lu, Q. Y.; Feng, G.; Komarneni, S. *J. Am. Chem. Soc.* **2004**, *126*, 54.
(22) Feng, G.; Lu, Q. Y.; Komarneni, S. *Chem. Commun.* **2005**, 531.
(23) Wang, H.; Zhu, J. J.; Zhu, J. M.; Chen, H. Y. *J. Phys. Chem. B* **2002**, *106*, 3848.
(24) Liao, X. H.; Wang, H.; Zhu, J. J. *Mater. Res. Bull.* **2001**, *36*, 2339.
(25) Sigman, M. B., Jr.; Korgel, B. A. *Chem. Mater.* **2005**, *17*, 1655.

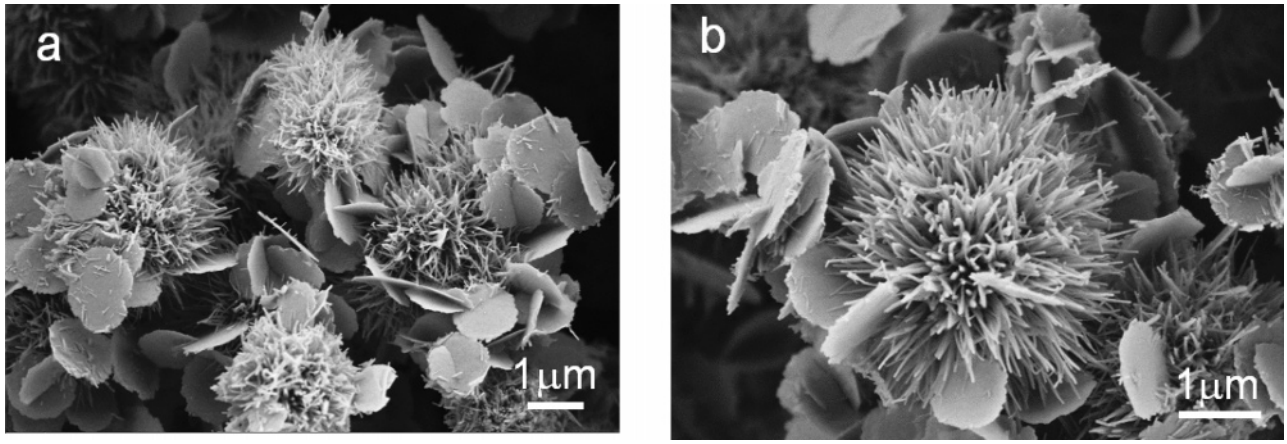

Figure 2. SEM images of the products obtained in the ionic liquid system after reaction at 120 °C for 1 h. Starting pH = 4.

L). Then, the mixture was put in an oven at 120 °C for 20 h. The gray-black precipitate that formed was collected by centrifugation of the mixture and then washed with dilute water and ethanol three times, respectively. Similarly, intermediate products obtained at different temperatures were also produced and collected.

2.3. Characterization. X-ray diffraction (XRD) analysis was performed on a Rigaku (Japan) D/max-γ_A X-ray diffractometer equipped with graphite-monochromatized Cu Kα radiation (λ = 1.541 78 Å). The TEM images were taken with a Hitachi model H-800 transmission electron microscope, with an accelerating voltage of 200 kV. High-resolution transmission electron microscope (HRTEM) photographs and selected area electron diffraction (SAED) patterns were obtained on a JEOL-2010 transmission electron microscope. X-ray photoelectron spectroscopy (XPS) was carried out on an Escalab M KII X-ray photoelectron spectrometer with Mg Kα X-rays as the excitation source. UV−vis absorption spectrum was recorded with a Shimadzu UV-2501 spectrophotometer in the wavelength range of 200−800 nm at room temperature.

The structure of the ionic liquid solution was detected by laser light scattering (LLS) on ALV-5000E with a He−Ne laser (λ_0 = 632 nm) as the source at 298 K. The ionic liquid solution was diluted to 5.0 $\times 10^{-3}$ g/mL and was filtered through a 0.5 mm Millipore Millex-LCR filter to remove dust before the LLS experiments. The root-mean-square radius of gyration $\langle R_g \rangle$ and the hydrodynamic radius (R_h) of the micelles were determined by static and dynamic LLS, respectively.

3. Results and Discussion

3.1. Phase Transformation. Figure 1 shows the time-dependent XRD patterns of Bi_2S_3 nanostructures obtained at 120 °C. The XRD pattern in Figure 1a indicated that the peaks are very broad and can be indexed as a mixture of Bi_2S_3 phase and an impurity phase. This impurity phase can be indexed as to the tetragonal structure BiOCl, which corresponds to the standard values (JCPDS Card 06-0249).[28] When the reaction time was prolonged up to 3−6 h, the BiOCl phase vanished and the peaks became stronger gradually (Figure 1b). When reaction time reached 20 h, the diffraction peaks are very narrow and strong, indicating that the crystallinity was much improved. All the peaks could be indexed as the orthorhombic Bi_2S_3 with cell constants of a = 10.73, b = 11.30, and c = 3.98, which are consistent with the standard values (JCPDS Card 17-0320).[19,20]

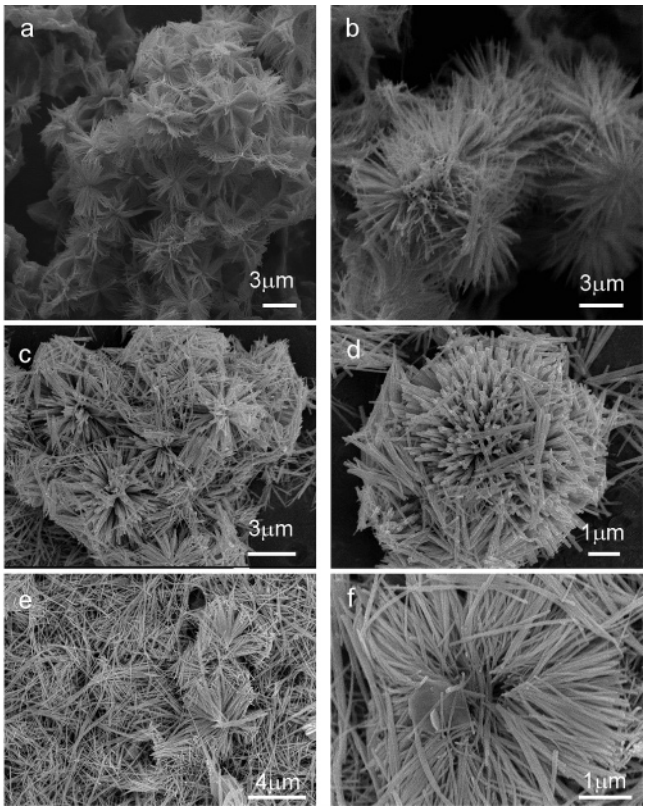

Figure 3. SEM images of the products obtained in an ionic liquid system after reaction for different time at 120 °C: (a, b) 3 h; (c, d) 6 h; (e, f) 20 h. Starting pH = 4.

The following chemical reactions occurred in the formation of Bi_2S_3 product:

$$BiCl_3 + H_2O \rightarrow BiOCl + 2HCl$$

$$CH_3CSNH_2 \xrightarrow{H^+} H_2S + CH_3N$$

$$Bi^{3+} + H_2S \rightarrow Bi_2S_3 + 3H^+$$

3.2. Morphogenesis of Bi_2S_3. The shape evolution of the products obtained after reaction for different times was

(26) Jiang, Y.; Zhu, Y.-J. *J. Phys. Chem. B* **2005**, *109*, 4361.
(27) Wilkes, J. S.; Zaworotko, M. *J. Chem. Commun.* **1992**, 965.
(28) Joint Committee on Powder Diffraction Standards. Diffraction Data File 06-0249.

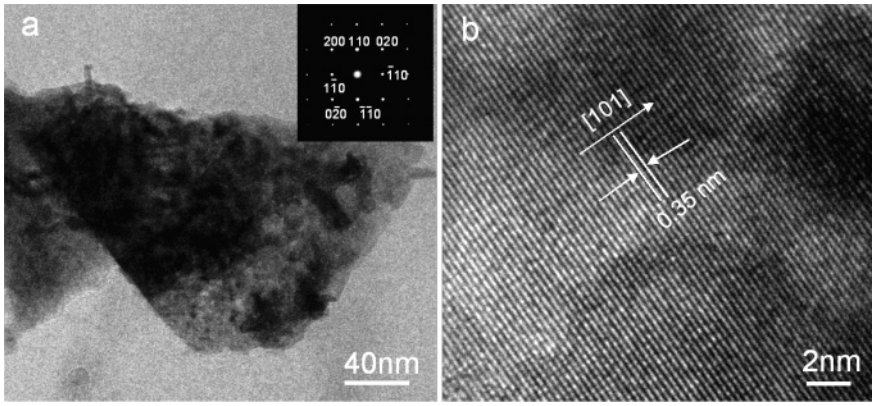

Figure 4. HRTEM images of the nanosheets obtained in an ionic liquid system after reaction for 1 h at 120 °C. Starting pH = 4. (a) TEM image of a typical BiOCl nanosheet. (Inset) Corresponding electron diffraction pattern (SAED) taken on the nanosheet along the ⟨001⟩ zone. (b) Typical HRTEM image taken on an individual BiOCl nanosheet.

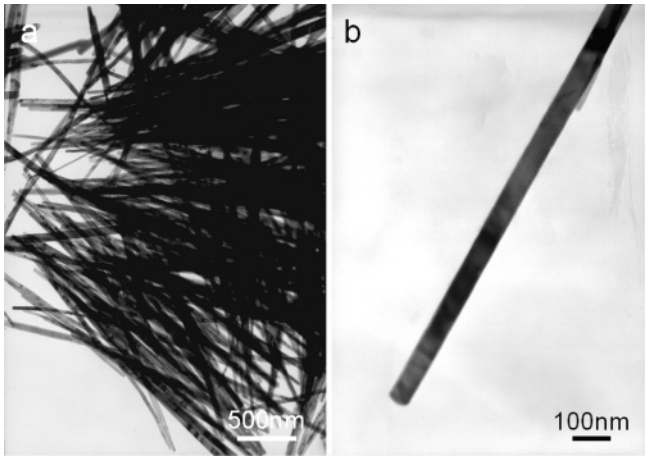

Figure 5. TEM images of the sample obtained in the ionic liquid system after reaction at 120 °C for 3 h. The sample was observed after ultrasonic treatment.

examined by transmission electron microscopy (TEM) and scanning electron microscopy (SEM) (Figures 2 and 3). At the primary stage before reaction, the mixed solution was yellow in the ionic liquid system and brown after sonochemical treatment for about 5 min. After the mixture was heated for 1 h, the yellow color gradually disappeared; a large amount of black precipitate was generated, and many nanorods and nanosheets can be observed (Figure 2a). From the combined analysis of the XRD pattern in Figure 1a and SEM image in Figure 2a, it can be concluded that the nanosheets belong to the BiOCl phase. To further confirm whether the nanosheets really belong to the BiOCl phase, the nanosheets were examined by the selected electron diffraction pattern and high-resolution transmission electron microscopy (HRTEM), as shown in Figure 4. The selected electron diffraction pattern taken along the [001] direction on an individual nanosheet (inset in Figure 4a) indicates that the BiOCl nanosheet is perfectly single crystalline. The well-resolved lattice fringes with a constant spacing of 0.35 nm corresponding to that of the (101) planes can be frequently observed, as shown in Figure 4b.

When the reaction was prolonged up to about 3 h, no sheetlike particles are observed anymore (Figure 1b) and all the particles are in the form of spherical flowers composed of nanowires (Figure 3a,b). Figure 5 shows the TEM images of the product after ultrasonic treatment during preparation of the TEM sample. The nanowires are straight with a diameter of 50 nm and length up to 2 μm (Figure 5a). A typical nanorod is shown in Figure 5b.

When the reaction time is prolonged up to 6 and 20 h, respectively, the rods became thick and rigid. These nanorods are usually several micrometers long with diameters about 70−80 nm (Figure 3c−f). With prolonged reaction time, many individual nanowires fell off the flowers (Figure 3c,e). The number of individual nanowires is increased with prolonged the reaction time (Figure 3c−f). Figure 3f shows a typical nestlike structure with a hollow core. The formation mechanism of flowerlike structures will be discussed later.

Effect of pH on the Bi_2S_3 Crystallization. The pH value of the reaction medium plays a key role in the present procedure for the synthesis of Bi_2S_3 nanoflowers. First, a suitable pH value can effectively prevent $BiCl_3$ hydrolysis to BiOCl in the initial reaction stage and kinetically control the growth rate of dendrite Bi_2S_3 nanostructures. When the pH value is about 2, even within a short period, for example, about half an hour, large-scale and uniformly shaped Bi_2S_3 nanoflowers with a size of 3∼5 μm can be prepared conveniently (Figure 6). However, as the pH value increases up to 4, a large amount of BiOCl nanosheets still can be observed even after reaction for 1 h (Figures 1a and 2).

A high-resolution transmission electron microscope image taken on an individual nanowire in Figure 7 indicated that the nanowire is single crystal. Lattice resolved fringes with a constant spacing of 0.79 nm corresponding to that of the (110) planes (Figure 7b) can be clearly observed, which are parallel to the nanowire axis. And it can be inferred that the growth direction of the nanowire is along the *c* axis, which is confirmed by the selected area diffraction pattern (inset, Figure 7a). The EDX analysis on the local area of the sample shown in Figure 7c suggested the atom ratio of Bi:S is 1:0.69, indicating that S is slightly in excess compared to Bi. The peaks of Cu and C come from the TEM copper grid. The growth direction of the Bi_2S_3 nanowires is different from that found for Bi_2S_3 nanostructures by other synthetic methods reported previously.[20,25,26]

Templating Mechanism of Bi_2S_3 Flowers. The formation mechanism of Bi_2S_3 flowers is obviously due to a templating effect in the present ionic liquid− water reaction system. Transmission electron microscope (TEM) image (Figure 8)

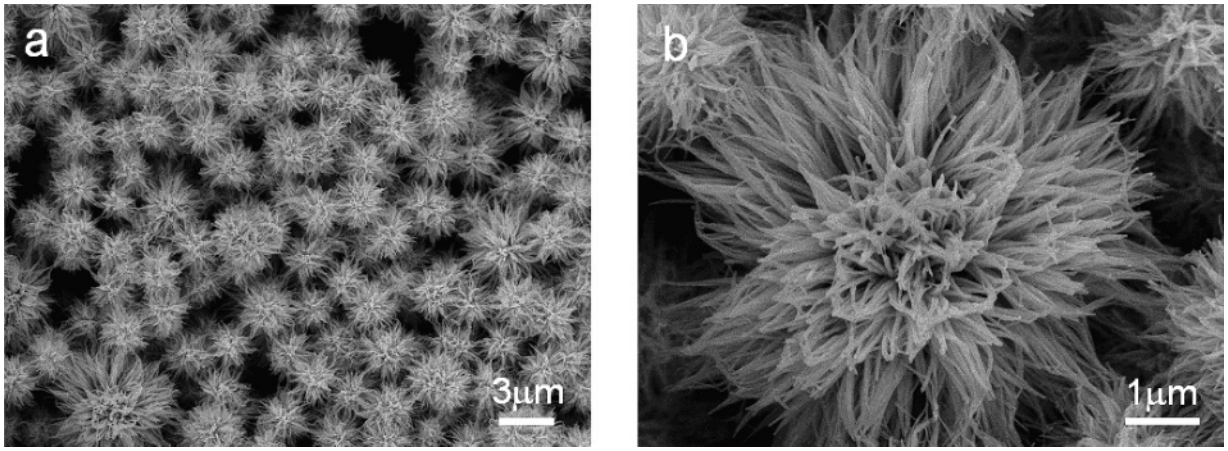

Figure 6. SEM images of the product obtained in an ionic liquid system after reaction at 120 °C for 0.5 h. Starting pH = 2.

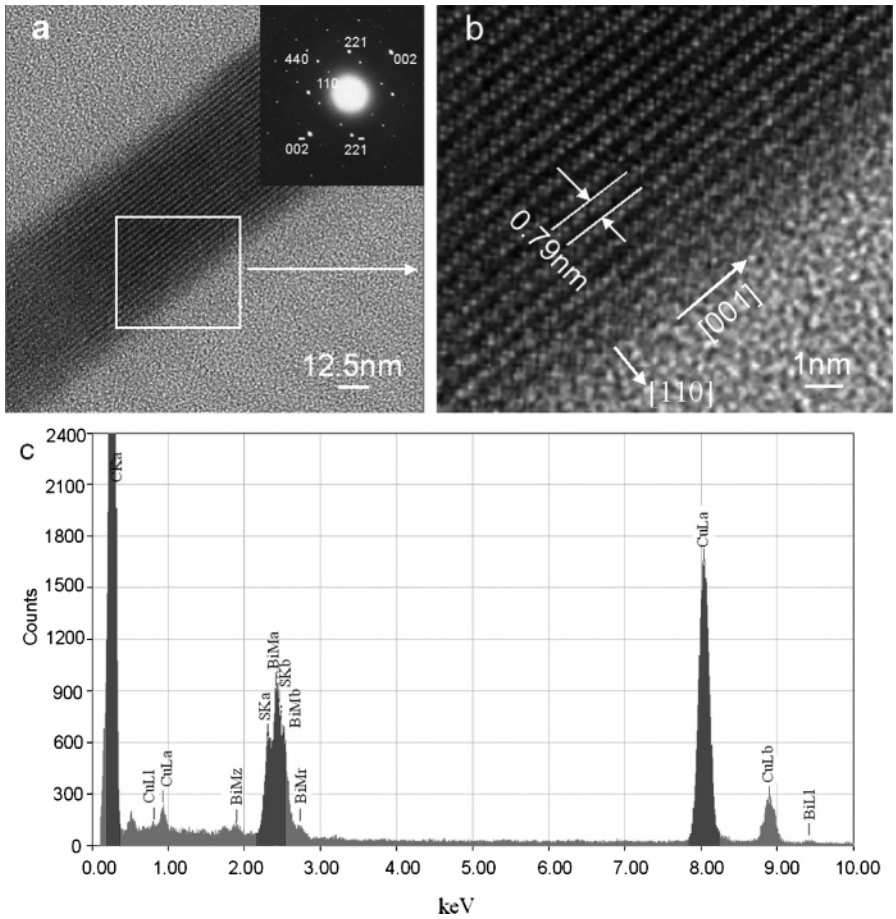

Figure 7. (a) HRTEM image of an individual Bi_2S_3 nanorod. (Inset) Corresponding electron diffraction pattern (SAED) taken on the nanorod. (b) Magnified image of a selected area marked in panel a. (c) Corresponding EDX spectrum taken from the nanorod shown in panel a.

for a diluted ionic liquid solution (5.0×10^{-3} g/mL) shows that there are a large number of vesicles with a size of about 200 nm. Hydrodynamic radius distribution of the ionic liquid solution in water has been done at room temperature (293 K) with scan angle $\theta = 15°$. Figure 9 shows the average hydrodynamic radius of the ionic liquid is $\langle R_h \rangle = 159$ nm and a hydrodynamic radius distribution $f(R_h)$, which can be calculated by use of the Stokes−Einstein equation:

$$R_h = (k_B T/6\pi\eta)D^{-1}$$

where k_B, T, and η are the Boltzmann constant, the absolute temperature, and the solvent viscosity, respectively. On the other hand, static LLS shows $\langle R_g \rangle = 157$ nm. The ratio $\langle R_g \rangle / \langle R_h \rangle$ can reflect the structure of a particle.[29] The ratio of $\langle R_g \rangle / \langle R_h \rangle \sim 0.99$ further indicates that the vesicles were formed in the ionic liquid solution.

Above analysis demonstrated that uniform Bi_2S_3 flowers are indeed templated from the vesicles existing in the present reaction system. The whole formation process of Bi_2S_3 flowers in the ionic liquid can be proposed as illustrated in Scheme 2. At the beginning, the vesicles are formed in the solution. Due to the hydrophobicity of $[BMIM]^+$ and the

(29) Burchard, W.; Schmidt, M.; Stockmayer, W. H. *Macromolecules* **1980**, *13*, 1265.

Scheme 2. Illustration of the Formation Mechanism of Bi_2S_3 Flowers in Ionic Liquid Solution

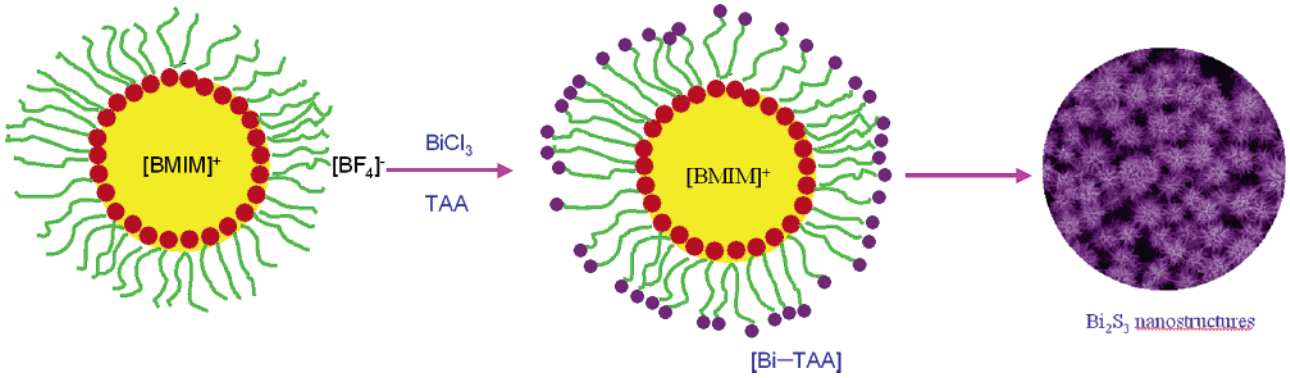

hydrophilicity of $[BF_4]^-$, the hydrophilic $[BF_4]^-$ groups will be outside the vesicles. With addition of the reactants $BiCl_3$ and TAA, the solution will become yellow, indicating the formation of [Bi-TAA] complex. [Bi-TAA] complex in the solution will be associated with $[BF_4]^-$ groups. Then Bi_2S_3 will start to crystallize on the surface of these vesicles. The preferential growth of Bi_2S_3 into nanorods/nanowires depends on its intrinsic nature as reportedly previously.[19] Therefore, the balllike flowers composed of nanowires can be constructed. At the initial stage, uniform flowers will form and the nanowires are packed in a radial way with dense structures (Figure 5a). The radial growth pattern observed here could be under control of some forces that act perpendicular to the fiber axis and control their interspacing, as we reported previously in the formation of $BaCrO_4$ and $BaSO_4$ fiber superstructures under control of a double

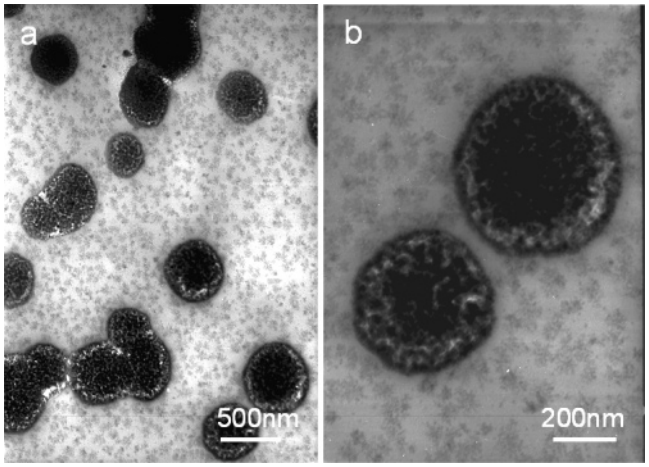

Figure 8. TEM images of the vesicles formed in the ionic liquid solution with a concentration of 5.0×10^{-3} g/mL.

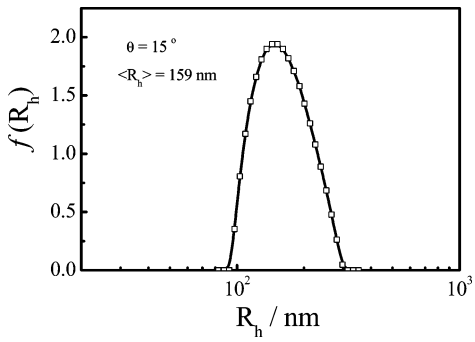

Figure 9. Hydrodynamic radius distribution of the ionic liquid solution in water. The concentration is 5.0×10^{-3} g/mL.

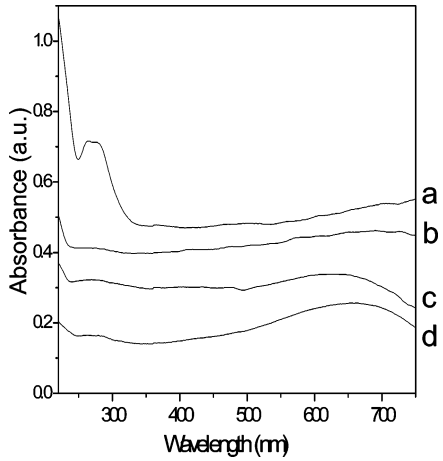

Figure 10. UV−Vis absorbance spectra of Bi_2S_3 nanostructure prepared at 120 °C for (a) 1 h, (b) 3 h, (c) 6 h, and (d) 20 h.

hydrophilic block copolymer or a simple polyelectrolyte.[30] With prolonged reaction time, the nanowires grow further and spread out in different directions but in a radial way. The bigger nanowires grew and the thinner nanofibers vanished according to the Ostawald ripening process. The loose structures of spheres with incomplete spherical shape appeared with prolonged time, and also the individual nanowires fell off from the mother spherical structures. All these phenomena suggested that the forces between the nanowires became weaker and weaker with prolonged reaction time and finally are not strong enough to hold the spherical structures anymore.

UV−Vis Absorption Spectral Analysis of the Bi_2S_3 Nanostructures. The UV−vis absorption spectra for the products synthesized by this approach with different reaction times are shown in Figure 10. The products after 1 h shows a broad absorption peak at 270 nm corresponding to the band gap of 4.59 eV (Figure 10a), which is quite similar to that synthesized by a photochemical synthesis method.[31] With increasing times of 3, 6, and 20 h, the peak at 270 nm became weak little by little and disappeared at last (Figure 10b−d). Peaks at 672 nm (1.85 eV) and 689 nm (1.80 eV) appeared for the products obtained after reaction for 6 and 20 h,

(30) (a) Yu, S. H.; Cölfen, H.; Antonietti, M. *Chem. Eur. J.* **2002**, *8*, 2937. (b) Qi, L.; Cölfen, H.; Antonietti, M.; Li, M.; Hopwood, J. D.; Ashley, A. J.; Mann, S. *Chem. Eur. J.* **2001**, *7*, 3526. (c) Yu, S. H.; Antonietti, M.; Cölfen, H.; Hartmann, J. *Nano Lett.* **2003**, *3*, 379.
(31) Zhao, W. B.; Zhu, J. J.; Zhao, Y.; Chen, H. Y. *Mater. Sci. Eng. B* **2004**, *11*, 307.

respectively (Figure 10c,d), which are similar to those reported previously by Liu et al.[19c] All the band gaps obtained are shifted to higher energy compared to the typical direct band gap of 1.3 eV of Bi_2S_3.

Conclusion

In summary, Bi_2S_3 flowers composed of uniform nanowires have been successfully prepared in high yield via an ionic liquid-assisted reaction system at low temperature and ambient atmosphere. Laser light scattering (LLS) experiments indicated that vesicles with a size of 200−500 nm formed in diluted solutions of ionic liquid with deionized water, which act as templates for the formation of Bi_2S_3 flowers. Such flowerlike structures tend to become loose and fall off from the mother flowers, and finally the individual nanowires will form. The reaction time, reaction temperature, and pH value also had important influences on controlling the morphology of the particles. This approach opens a new method for the morphogenesis and crystallization of Bi_2S_3 material and could be rapidly extended for the synthesis of other inorganic nanomaterials such as metal chalcogenide semiconductors with novel morphology and complex form.

Acknowledgment. We appreciate funding support from the Centurial Program of the Chinese Academy of Sciences, the National Science Foundation of China (20325104, 20321101, and 50372065), the Scientific Research Foundation for Returned Overseas Chinese Scholars, and State Education Ministry. We also thank Professor Markus Antonietti in the Max Planck Institute of Colloids and Interfaces for his genuine support of the ongoing ionic liquid templating project, which is partially supported by the Partner-Group of Max Planck Society−Chinese Academy of Sciences.

CM051632T